Functional Materials 14, No.1 (2007)

Thermostimulated implantation of nanoscaled Ag particles into a quartz glass using a CO_2 laser beam

L.A.Ageev, V.K.Miloslavsky, E.D.Makovetsky, K.S.Beloshenko, A.V.Stronsky[*]

Physical Optics Chair, V.Karazin Kharkiv National University, 4 Svobody Sq., 61077 Kharkiv, Ukraine
[*]V.Lashkaryov Institute for Semiconductor Physics, National Academy of Sciences of Ukraine, 45 Nauki Ave., 03028 Kyiv, Ukraine

Received September 9, 2006

Coloration of fused quartz with colloidal silver (particle radius $a \approx 3$ nm) is realized by irradiation of thin (≈10 nm) granularr Ag film on a quartz plate by a continuous Gauss beam of CO_2 laser ($\lambda = 10.6$ μm, $P = 30$ W). Using the AFM microscopy, a relief of the colored surface has been revealed. It is formed by oval lugs with mean transversal size of about ≈ 0.2 μm and heights of several nanometers. The relief is created due to surface deformation caused by subsurface Ag granules. The measured absorption spectrum of the colloid has shown that the absorption band contour is similar to the Lorentz one, maximum being at $\omega_m = 4.48 \cdot 10^{15}$ s^{-1}, and half-width is $\gamma = 0.714 \cdot 10^{15}$ s^{-1}. Making use of Maxwell-Garnet theory, it has been found that for this colloid, the filling factor is $q \approx 0.05 \div 0.10$ and coloration depth $h \approx 100 \div 50$ nm.

Реализовано окрашивание плавленого кварца коллоидным серебром (радиус частиц $a \approx 3$ нм) путем облучения тонкой (≈10 nm) островковой пленки Ag на поверхности кварцевой пластины непрерывным гауссовым пучком CO_2-лазера ($\lambda = 10.6$ мкм, $P = 30$ Вт). С помощью АСМ-микроскопа обнаружен рельеф окрашенной поверхности, образованный выступами овальной формы со средним поперечным размером ≈ 0.2 мкм и с высотой в несколько нанометров; рельеф создан в результате деформации поверхности образовавшимися под поверхностью гранулами Ag. Измеренный спектр поглощения коллоида показал, что контур полосы поглощения близок к Лоренцеву, максимум находится на частоте $\omega_m = 4.48 \cdot 10^{15}$ с$^{-1}$, полуширина равна $\gamma = 0.714 \cdot 10^{15}$ с$^{-1}$. С помощью теории Максвелла-Гарнета найдено, что коллоиду соответствует фактор заполнения $q \approx 0.05 \div 0.10$ и глубина окрашивания $h \approx 100 \div 50$ нм.

At present, the interest in the problem of coloration of dielectrics by tiny metal particles is associated with development of nonlinear optics and optics of nanoscaled structures [1, 2]. The monography [1] contains a review of works (approximately till 1995) on optical properties of metal clusters in dielectrics and, in particular, it is noticed that implantation of metal particles in quartz glass is a rather difficult task. The only way mentioned in [1] is joint evaporation of metal and quartz in vacuum [3]. Recently, this problem is being solved by use of specially prepared porous quartz glass, the particles being implanted into it by chemical way [4]. In this work, it is shown that it is possible to implant minute colloidal Ag particles into a thin surface layer of quartz glass by treating a thin Ag film on quartz by a CO_2 laser beam, the

film being deposited by silver evaporation in vacuum. The absorption band of colloid is measured and analyzed using the theory of optical properties of small absorbing particles implanted in a dielectric [1, 5].

In the experiment, we used polished plane-parallel quartz plates of 2 mm thickness and 10 cm^2 area. A thin (about 10 nm) Ag film was deposited onto the unheated quartz surface under vacuum ($5 \cdot 10^{-5}$ mm Hg). The films of such thickness are known to have an granular structure [6]. The plate with Ag film then was irradiated in air with a Gauss beam of CO_2 laser ($\lambda = 10.6$ μm, $P = 30$ W, the beam effective diameter 3 to 4 mm). Researches of thermal action of such a beam on absorbing media had shown that it can heat up surfaces of various samples to temperatures of 900° to 1200°C.

The absorption coefficient of the quartz glass at $\lambda = 10.6$ μm is $\alpha \approx 400$ cm^{-1} [7], i.e. the beam attenuation depth of $\alpha^{-1} \approx 25$ μm is much smaller than the quartz plate thickness. Therefore, the beam is completely absorbed in quartz. The temperature of heated surface may be judged from the glow brightness at irradiated site of the sample and determined by pyrometric measurements of the brightness temperature. However, the quartz plate heating does not result in any glow of the irradiated site, since the radiant emittance of quartz in the visible spectral range is low. Measurements at the plate back side using a chromel-alumel thermocouple have shown that the temperature is $T \approx 600$°C. The front surface of plate can be assumed to be heated up to $T \approx 1000$°C. Then at linear approximation of T decrease along the beam axis Z and at plate thickness $\Delta Z = 2$ mm the temperature gradient is $dT/dZ \approx 200$°C/mm.

Under irradiation, noticable changes are first observed in the deposited film. It is seen that the film becomes quickly colored yellow in a circular zone surrounding the acting beam. This coloration spreads in radial directions far from the beam center. The coloration is associated with the film structure transformations caused by thermal diffusion processes. During heating, the film on quartz becomes a two-dimensional colloid and starts to absorb light according to the known mechanism of plasma resonance [5].

After approximately 1 min, a visible glow appears in the area of laser beam action. The glow quickly becomes nearly white. Pyrometric measurements have shown that the color temperature is approximately 960°C. The actual temperature is somewhat higher than the color one, so the film is heated up to the temperature higher than the silver melting temperature $T_{melt} = 960.8$°C. It is well known that about 10 nm thick granular Ag films have a large absorbing ability (30 to 35 % [5]). This is why the bright thermal glow appears in the heated film. Further irradiation leads to gradual disappearance of the visible glow in the center of irradiated area. The glowing area becomes a slowly expanding ring. At large exposition, the glow in central area disappears completely, and the glowing ring reaches its maximum diameter.

In further researches, we used the samples irradiated till appearance of bright glow in central area. After irradiation, the sample was immersed in sulfuric acid solution to remove Ag from the quartz surface. The silver particles in quartz are protected against acid and at normal conditions remain fixed as long as we want. The area of the film where Ag is penetrated into quartz has a diameter of 3 to 4 mm and looks yellow in transmitting light. In reflected white light, one may often see an interference coloration. Under bright illumination, a blue scattering is always seen. Visual observations also show that silver is distributed inhomogeneously over the irradiated area. Perhaps the inhomogeneity due to fluctuations in azimuthal dependence of transversal temperature gradient $\Delta T(X,Y)$.

Typical examples of areas with introduced silver are shown in Fig. 1. The photograph was made in reflected light. Fig. 1a demonstrates the area irradiated till the glow appearance in the central part of irradiated area. This film was used in further researches. Fig. 1b demonstrates the circular zone formed by introduced silver at large exposition under laser beam.

Implantation of silver must disrupt the polished quartz surface. However, the surface damage magnitude is less than visible light wavelengths, since there is no scattering in the visible spectral range. We irradiated the film by a thin He–Ne laser beam ($\lambda = 633$ nm) and did not notice any spatial distortions of both reflected and transmitted beam at its incidence on colored area. But the reflected beam intensity at normal incidence increases considerably as compared to reflection from pure quartz surface. This evidences a higher refractive index of the colored area.

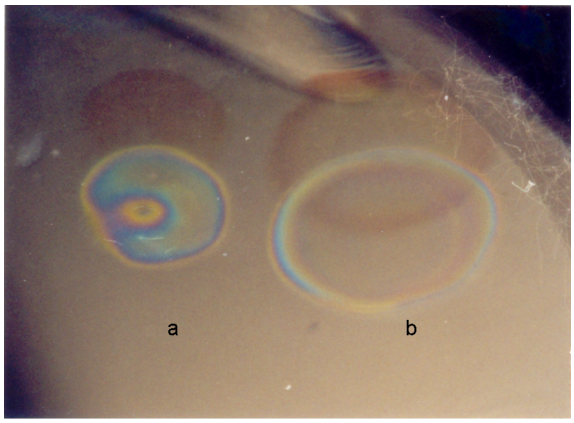

Fig. 1. Photographs of the colored areas in reflected white light: (a) the area where irradiation by CO_2 laser beam was stopped during the stage of white glow. Difference in interference coloration indicates inhomogeneous Ag distribution; (b) the area shaped as colored ring after large exposure to irradiation. Shadows from colored areas on the back side of quartz plate are also seen.

The surface of colored area was studied using transmission electron microscopy (using a replica separated from the surface after shadowing by a thin golden film) and atomic force microscopy (AFM). Both methods allowed to reveal the surface relief. The AFM provides a more detailed, three-dimensional picture of the relief (Fig. 2a). The relief is seen to be a set of chaotically alternating lugs and valleys. The bright parts of the relief at Fig. 2 are lugs. Detailed AFM analysis (Fig. 2b) has shown that in projection on X, Y plane, the ascending elements have mostly elliptical or rounded shape. There are also clusters of relatively small, contacting elements. The mean size of individual elements is approximately 0.2 μm. Individual ascending elements have roughed surface and small heights. Analysis of the relief magnitude along Z axis shows that the magnitude fluctuates within several nanometers (Fig. 2b).

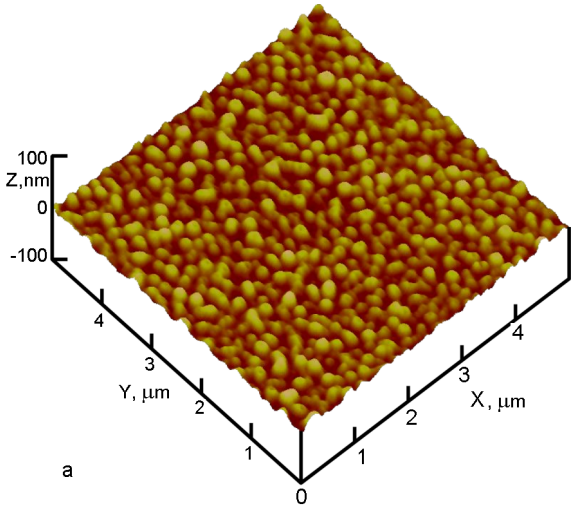

Fig. 2. AFM photographs of the surface of colored quartz area: (a) scale along both X- and Y-directions is 1 μm per division, scale along vertical Z-axis 100 nm per division; (b) analysis of the area approximately 1×1 μm^2, change of the relief amplitude along the line with colored triangles is shown in the graph. Horizontal axis corresponds to this line, Z-axis is vertical. Triangles indicate coordinates of several points. Distance between green triangles along horizontal line of scanning is 90.3 nm, between red ones, 66.6 nm, between black ones, 90.1 nm. Distance between green triangles along Z-axis is 7.7 nm, between red ones, 4.8 nm, between black ones, 3.2 nm. The green and red triangles indicate a "crater" on a ascendent element of the relief.

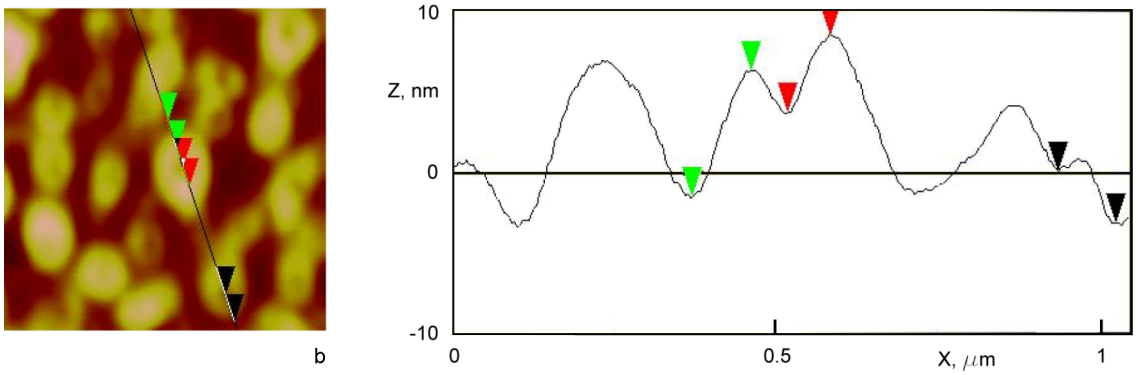

Often there are "craters" in central parts of ascending elements.

The relief must be a result of quartz surface deformation with Ag particles situated mainly immediately under the surface. The photograph of quartz surface does not allow to judge the sizes of particles and their depth distribution. It is only a picture of the relief generated at quartz surface as a result of Ag implantation. An important information on the structure of quartz layer colored with Ag can be obtained from its optical characteristics. The optical properties of colored area were studied using the transmission spectrum $T(\lambda)$ measurements by an SF-16 spectrophotometer. The measuring beam of SF-16 was restricted using an aperture so its diameter was somewhat smaller than the colored area diameter. The measurements were carried out in the wavelength range $\lambda = 270 \div 620$ nm. The range includes a colloidal absorption band of Ag and an edge of interband absorption. The measured results are shown in Fig. 3 as experimental points in the dependence of optical density $D = -\ln(T)$ on frequency $\omega = 2\pi c/\lambda$.

The coloration of quartz with Ag granules is obviously associated with strong heating of the surface and the film thereon. As to the coloration mechanism, the following can be said. Surface temperature reaching the melting temperature of silver, an electron emission from melted Ag particles to quartz must arise. The electrons are captured with traps in quartz, and Ag particles become positively charged. This results in an electrostatic field causing separation of Ag^+ ions from particles and ion transfer to the traps. Such process is repeated many times and finally results in formation of minute Ag granules in surface layer of quartz. The granule formation in fused quartz is favored by its "porosity". The porosity degree may be determined from the ratio of fused quartz density to crystal quartz one. The ratio is 0.83. This mechanism is similar to the mechanism of polycrystalline AgCl film coloration by colloidal Ag particles [8], but in the latter case, free electrons appear not due to thermoelectronic emission, but to photoeffect in the thin Ag film covering the AgCl film.

The assumed coloration process takes place during initial stage of exposure when temperature of the central part of irradiated site reaches T_{melt}. The heated Ag particles produce a visible glow. Then the glow in the center of irradiation disappears, the glowing area becomes a ring, the dark central area gradually widens, and the ring diameter increases along with decrease of its width. Apparently such transformations are associated with removal of Ag from the quartz surface in the central area, and with gradual T increase in directions transverse to the laser beam. Such a time-dependent large-scale irregularity of coloration corresponds to a Gaussian beam. But thermal processes result in additional small-scale inhomogeneities seen as variations of interference coloration in Fig. 1.

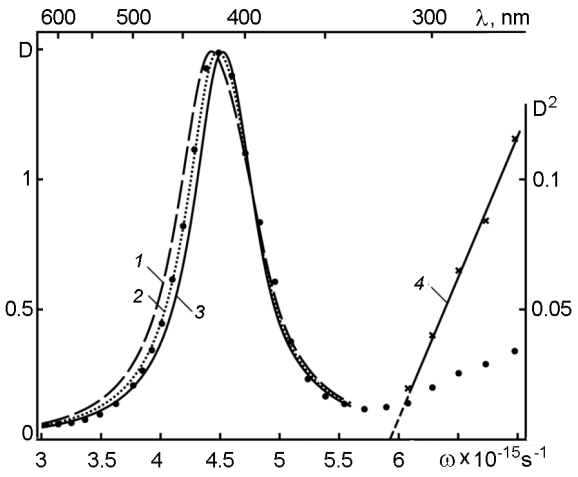

Fig. 3. Absorption spectrum $D(\omega)$ is shown as experimental points; *1*, *2*, *3*, calculated contours $D(\omega)$ for $q = 0.15$, 0.10, 0.05, *4*, experimental dependence $D^2(\omega)$.

The microrelief revealed by the AFM seems to arise in the following way. The Ag particle appearance in quartz should increase its volume and create internal stresses. If the particle is situated immediately under the surface, a lug should appear on the surface. The lug shape and size are somehow connected with the particle shape and size. As projections of the lugs on surface are oval (Fig. 2), one can consider that those are formed by Ag granules of a nearly spherical form. As to the granule radius, it can be assumed to be equal to the corresponding height of lug. The radii do not exceed several nanometers. The "craters" observed in many lugs may appear at cooling-down of the melted particles and their crystallization. This results in the particle volume reduction and partial relaxation of quartz deformation mainly nearby the lug center.

Analysis of the experimental colloidal absorption band allows to obtain important information on structure of colloidal Ag solution formed in quartz. Experimental points (Fig. 3) reveal that the absorption band has

a bell-like shape. The band is essentially symmetrical. The maximum optical density is $D_m = 1.49$, it corresponds to frequency $\omega_m = 4.48 \cdot 10^{15}$ s^{-1} ($\lambda_m = 420.5$ nm). The band half-width is $\gamma = 0.714 \cdot 10^{15}$ s^{-1}. The band is found to be approximable by Lorentz contour (not shown in Fig. 3).

$$D = D_m \frac{\gamma^2}{4[(\omega - \omega_m)^2 + \gamma^2/4]}. \quad (1)$$

The Lorentz contour indicates a uniform broadening of the absorption band. The uniform broadening may be created by minute non-interacting granules of nearly equal sizes. In this case, the frequency ω_m must met the Froehlich formula [9]: $\omega_m \approx \omega_F$ where

$$\omega_F = \frac{\omega_p}{\sqrt{\varepsilon_M + 2\varepsilon_0}}, \quad (2)$$

where ω_p is the plasma frequency. It is not known precisely. According to the data reported by various authors, value of this frequency is within limits of $(13 \div 13.9) \cdot 10^{15}$ s^{-1}. To calculate ω_F, we have used the mean value $\omega_p = 13.4 \cdot 10^{15}$ s^{-1}. Further, ε_M is the dielectric permittivity defined by interband transitions in a metal. Data on $\varepsilon_M(\omega)$ dispersion in Ag are provided in [10] (see Table), whence $\varepsilon = 4.5$ for ω_m. Finally, ε_0 is the dielectric constant equal to squared refractive index of the medium containing the metal colloid. At ω_m frequency, the fused quartz has $\varepsilon_0 = 2.15$. Calculation using (2) at the listed data results in $\omega_F = 4.52 \cdot 10^{15}$ s^{-1}. It is in a rather well agreement with experimental ω_m value. The agreement between experimental and calculated values evidences the validity of the colloid description as a system of minute non-interacting Ag particles in quartz matrix.

For Ag, the threshold frequency ω_{thresh} is known. Starting from this frequency, the light absorption is associated with direct interband transitions. Measurements presented in Fig. 3 include the edge of interband absorption. For direct transitions, the dependence $D^2(\omega)$ must be linear, and such a linearity occurs in fact. Intersection of this straight line with the ω axis results in known value $\omega_{thresh} \approx 5.9 \cdot 10^{15}$ s^{-1} [1]. Coincidence of experimental value ω_{thresh} and threshold value of the massive silver denotes absence of a quantum size effect in spite of small granule size. Besides, the constancy of interband absorption threshold allows us to use the dispersion of massive silver ε_M [10] to describe the colloid properties.

The Maxwell-Garnet theory was developed during 1903–1905. It was the first quantitative theory describing the properties of colloidal solutions [5]. It is based on the concept of minute metal particles in a dielectric as dipoles. Such a composite medium should evince properties of usual dielectric but with different optical constants. In our case, spherical Ag particles are distributed in quartz surface layer of a certain thickness. This thickness exceeds considerably the mean granule radius and a mean intergranular distance. Therefore, the colloid should be treated as three-dimensional one, so it meets the theory conditions. At the same time, the colloidal layer should have a sharply defined boundary with pure quartz, because otherwise the interference coloration (Fig. 1) could not be observed. Determination of the colloidal layer thickness is an interesting but uneasy problem. The Maxwell-Garnet theory allows us to determine optical characteristics of the studied colloid as well as to estimate reasonably its thickness.

The Ag granules form the colloidal layer due to thermal diffusion of electrons and Ag ions along the laser beam. In general, these granules should be distributed inhomogeneously in the layer. But even in that case, the granule distribution may be characterized by mean filling factor $q = N \times V$ where V is the mean volume of single particle and N is the particle concentration in the colloidal layer.

Table. Values of $\varepsilon_M(\omega)$ — the contribution to dielectric permittivity for account of interband transitions. The table was compiled using the data from [10].

$\omega \cdot 10^{-15}$ s^{-1}	3.0	3.2	3.4	3.6	3.8	4.0	4.2	4.4
ε_M	4.0	4.05	4.1	4.15	4.2	4.25	4.35	4.5
$\omega \cdot 10^{-15}$ s^{-1}	4.5	4.6	4.8	5.0	5.2	5.4	5.6	
ε_M	4.6	4.65	4.8	5.0	5.1	5.2	5.3	

The Maxwell-Garnet formula connects optical constants of the granule metal with effective optical constants of the colloid [1, 5]:

$$\frac{\varepsilon_{ef} - \varepsilon_0}{\varepsilon_{ef} + 2\varepsilon_0} = q\frac{\varepsilon - \varepsilon_0}{\varepsilon + 2\varepsilon_0}, \qquad (3)$$

where ε is the complex dielectric permittivity of the metal particle: $\varepsilon = \varepsilon_1 - i\varepsilon_2$, $\varepsilon_1 = n^2 - \chi^2$, $\varepsilon_2 = 2n\chi$, n and χ are the metal optical constants; $\varepsilon_{ef} = \varepsilon_{1ef} - i\varepsilon_{2ef}$ is the complex dielectric permittivity of the colloid. The formula (3) is interpolational one, and $\varepsilon_{ef} \to \varepsilon$ at $q \to 1$ while $\varepsilon_{ef} \to \varepsilon_0$ at $q \to 0$. The validity of (3) was verified by variuos researchers. For instance, in [11], the Mie theory based analysis was carried out, and it was shown that (3) takes into account the dipole-dipole interaction between particles and works for analysis of absorption spectra and reflection spectra at particle radii $a \leq 10$ nm.

To analyse the experimental absorption band, we should know ε_{ef} first of all. The formula (3) may be rearranged to make calculation of ε_{1ef} and ε_{2ef} more convenient:

$$\varepsilon_{1ef} = \varepsilon_0\left[-2 + \frac{3(1 - qB)}{q^2A^2 + (1 - qB)^2}\right]; \qquad (4)$$

$$\varepsilon_{2ef} = \frac{3\varepsilon_0 qA}{q^2A^2 + (1 - qB)^2},$$

where $A = \dfrac{3\varepsilon_0\varepsilon_2}{(\varepsilon_1 + 2\varepsilon_0)^2 + \varepsilon_2^2}$,

$$B = \frac{\varepsilon_1^2 + \varepsilon_2^2 + \varepsilon_1\varepsilon_0 - 2\varepsilon_0^2}{(\varepsilon_1 + 2\varepsilon_0)^2 + \varepsilon_2^2}.$$

To calculate the frequency dependences $\varepsilon_{1ef}(\omega)$ and $\varepsilon_{2ef}(\omega)$, we should know the dependences $\varepsilon_1(\omega)$ and $\varepsilon_2(\omega)$. The interband absorption edge for Ag lies in ultraviolet region while the absorption spectrum of Ag colloid in quartz is situated in visible spectral range. Therefore, the optical constants of Ag in visible range must be defined by free electrons, and we may use the Drude-Ziner formulae [12] taking into consideration $\varepsilon_M(\omega)$ — a contribution to ε from interband transitions:

$$\varepsilon_1(\omega) = \varepsilon_M(\omega) - \frac{\omega_p^2}{\omega^2 + \nu^2}, \qquad (5)$$

$$\varepsilon_2(\omega) = \frac{\omega_p^2\nu}{\omega(\omega^2 + \nu^2)},$$

where ν is the scattering frequency of electrons. It is known that $\nu = 4.5\cdot10^{13}\text{s}^{-1}$ for massive silver at room temperature [13]. However, the scattering frequency in small granules of mean diameter a is different from ν because of electron scattering at granule boundaries. The latter contributes essentially to the scattering frequency. The frequency of scattering at granule boundaries is specified by ratio of the electron speed at Fermi surface ν_F to the radius a. The resulting scattering frequency must coincide with half-width of experimental absorption band γ. For γ, we have

$$\gamma = \nu + \frac{\nu_F}{a}. \qquad (6)$$

This formula allows us to estimate the granule radius in colloid. It is known from [13] that $\nu_F = 2.3\cdot10^8$ cm·s^{-1}. Substituting γ, ν and ν_F in (6), we get $a \approx 3$ nm. This value meets the applicability conditions for the formulae (3, 4). The calculated a value is in agreement with the mean magnitude of oscillations of colored surface relief (Fig. 2b). Hence, the assumption of correlation between the magnitude and granule radii is confirmed.

When calculating ε from (5), one should use γ instead of ν. A theoretical treatment of the experimental absorption band $D(\omega)$ is aimed to get a calculated dependence of optical density $D(\omega)$ being in accordance with the experimental one. The calculations were carried out in the interval $\omega = (3 \div 5.6)\cdot10^{15}\text{s}^{-1}$ at $\gamma = 0.714\cdot10^{15}\text{s}^{-1}$. The table of $\varepsilon_M(\omega)$ values was used in calculations (Table compiling the used graphical data from [10]). Succession of $D(\omega)$ calculations is as follows. First, we calculate $\varepsilon_{12}(\omega)$ using the formulae (5). Second, we find $A(\omega)$ and $B(\omega)$ from (4). Then we calculate $\varepsilon_{1ef}(\omega)$ and $\varepsilon_{2ef}(\omega)$ using (4) at specified q. Thereafter, we calculate optical constants $n_{ef}(\omega)$, $\chi_{ef}(\omega)$ of the colloid using the formulae resulting from relations between n, χ and ε_1, ε_2:

$$\frac{n_{ef}(\omega)}{\chi_{ef}(\omega)} = \frac{1}{\sqrt{2}}\sqrt{\pm\varepsilon_{1ef}(\omega) + \sqrt{\varepsilon_{1ef}^2(\omega) + \varepsilon_{2ef}^2(\omega)}}. \qquad (7)$$

Using the obtained absorption index value $\chi_{ef}(\omega)$, we calculate the absorption coefficient $\kappa_{ef}(\omega)$:

$$\kappa_{ef}(\omega) = \frac{2\omega\chi_{ef}(\omega)}{c}, \quad (8)$$

where c is the light speed in vacuum.

Calculated and experimental $D(\omega)$ contours being coincident, optical density is production of the absorption coefficient and colloidal layer thickness h:

$$D(\omega) = \kappa_{ef}(\omega) \times h. \quad (9)$$

Basing on (9), we find h as ratio of experimental D value at ω frequency of D maximum to calculated κ_{ef} value at the same frequency. Then, knowing the h value, we calculate the whole absorption band contour. The $D(\omega)$ contours were calculated for three q values: $q = 0.15$; 0.10; 0.05 at $\omega_p = 13.6 \cdot 10^{15}$ s^{-1}. This ω_p value, as well as the value used in ω_F calculation with (2), is nearly in the middle of possible ω_p interval. The formula (2) is correct at very small particle size, i.e. at $q \to 0$, and calculation of band maximum location using (2) are less accurate as compared to calculation based on (3) and (5). When calculating the contour, q and ω_p were selected to give the best agreement with experiment both in maximum location and half-width. The calculation results are shown in Fig. 3. It is seen that the best agreement with experiment is for the contour at $q = 0.10$. Two other contours have deviations at the low-frequency slope of the band. The contour at $q = 0.15$ has an increased half-width and a maximum shifted noticeably to lower frequencies. At $q = 0.05$, the maximum nearly coincides with the experimental one, but half-width is somewhat decreased due to shift of the low-frequency slope. The high-frequency slopes practically coincide.

The coincidence of the experimental absorption band and calculated one at $q = 0.10$ may be accepted as the main result allowing to estimate the colloidal layer mean thickness. In this case, $\kappa_{ef} = 2.8 \cdot 10^{-5}$ cm^{-1} at the band maximum, and from (9), we obtain $h \approx 50$ nm. On the other hand, factor $q = 0.05$ can be also assumed if considering the inhomogeneous distribution of colloidal Ag in colored layer. At such q, there is $\kappa_{ef} = 1.5 \cdot 10^{-5}$ cm^{-1} at the band maximum. This gives $h \approx 100$ nm.

At the long-wave slope of the band ($\omega = 3 \cdot 10^{15}$ s^{-1}, $\lambda = 628$ nm), the absorption index decreases considerably ($\kappa_{ef} \approx 0.1 \cdot 10^{5}$ cm^{-1}) while the refraction index $n_{ef} \approx 1.8$ is much higher than that of pure quartz ($n \approx 1.46$). That is why the colored layer should be a dielectric with large n for red and near infra-red ranges and should have waveguide properties.

It is to note also that the considered method of silver implantation provides a thin colloidal layer with surface microroughness of quartz plate. Such a roughness may be used in experiments on amplification of luminescence of organic molecules deposited on the surface, and in experiments on giant Raman scattering [14].

To conclude, a coloration of fused quartz by colloidal silver (particle radii $a \approx 3$ nm) is realized by irradiation of a thin (≈10 nm) granular Ag film on a quartz plate surface by a continuous Gauss beam of CO_2 laser ($\lambda = 10.6$ μm, $P = 30$ W). Using AFM microscopy, a relief of the colored surface was revealed. It is formed by oval lugs of mean transversal size ≈0.2 μm and heights of several nanometers. The relief is created as a result of surface deformation due to Ag granules formed under the surface. The measured absorption spectrum of the colloid has shown that the absorption band contour is close to the Lorentz one, the maximum being at $\omega_m = 4.48 \cdot 10^{15}$ s^{-1}, the half-width is $\gamma = 0.714 \cdot 10^{15}$ s^{-1}. Making use of Maxwell-Garnet theory, it was found that for this colloid, the filling factor $q \approx 0.05 \div 0.10$ and coloration depth $h \approx 100 \div 50$ nm. The considered method of coloration may be used to mark the fused quartz products, to produce light filters and waveguide strips on its surface, and for experiments on giant Raman scattering observation.

We are thankful to colleagues of the NANU Center for collective use of devices at Institute for Semiconductor Physics of NANU "Diagnostics of semiconductor materials and device systems" for AFM measurements.

References

1. U.Kreibig, M.Vollmer, Optical Properties of Metal Clusters, Springer-Verlag, Berlin, Heidelberg (1995).
2. R.A.Ganeev, A.I.Resnyansky, A.L.Stepanov et al., *Optika i Spektr.*, **95**, 1034 (2003).
3. H.Hovel, S.Fritz, A.Hilder et al., *Phys. Rev.*, **B48**, 18178 (1993).
4. W.Cai, H.Hofmeister, T.Rainer, W.Chen, *J. of Nanoparticle Res.*, **3**, 443 (2001).
5. G.V.Rosenberg, Optics of Thin-Layer Coatings, GIFML, Moscow (1958) [in Russian].
6. L.A.Ageev, H.I.El-Ashkhab, *Zh. Prikl. Spektr.*, **60**, 152 (1994).
7. E.M.Voronkova, B.N.Grechushnikov, G.I.Distler, I.P.Petrov, Optical Materials for Infra-

Red Engineering, Reference Manual, Nauka, Moscow (1965) [in Russian].
8. L.A.Ageev, V.K.Miloslavsky, *Opt. Engin.*, **34**, 960 (1995).
9. C.F.Bohren, D.R.Huffman, Absorption and Scattering of Light by Small Particles, Wiley, New York (1983).
10. V.K.Miloslavsky, R.G.Yarovaya, *Optika i Spektr.*, **21**, 708 (1966).
11. W.T.Doyle, *Phys. Rev. B*, **39**, 9852 (1989).
12. M.M.Noskov, Optical and Magneto-Optical Properties of Metals, Sverdlovsk (1983) [in Russian].
13. V.G.Padalka, I.N.Shklyarevsky, *Optika i Spektr.*, **11**, 527 (1961).
14. Surface Enhanced Raman Scattering, ed. by R.Chang and T.Furtak, Plenum Press, New York and London (1982).

Термостимульована імплантація нанорозмірних часток Ag у кварцеве скло за допомогою пучка CO_2-лазера

Л.О.Агєєв, В.К.Милославський, Є.Д.Маковецький, К.С.Білошенко, О.В.Стронський

Реалізовано забарвлення плавленого кварцу колоїдним сріблом (радіус часток $a \approx 3$ нм) шляхом опромінення тонкої (≈ 10 нм) острівкової плівки Ag на поверхні кварцової пластини неперервним гаусовим пучком CO_2-лазера ($\lambda = 10.6$ мкм, $P = 30$ Вт). За допомогою АСМ-мікроскопу виявлено рельєф забарвленої поверхні, створений виступами овальної форми із середнім поперечним розміром ≈ 0.2 мкм та висотою в декілька нанометрів; рельєф створений у результаті деформації поверхні гранулами Ag, що сформувалися під нею. Виміряний спектр поглинання колоїду показав, що контур смуги поглинання є близьким до Лоренцевого, максимум знаходиться на частоті $\omega_m = 4.48 \cdot 10^{15}$ с$^{-1}$, напівширина дорівнює $\gamma = 0.714 \cdot 10^{15}$ с$^{-1}$. За допомогою теорії Максвела-Гарнета знайдено, що колоїду відповідає фактор заповнення $q \approx 0.05 \div 0.10$ та глибина забарвлення $h \approx 100 \div 50$ нм.